

IN-MEDIUM PROPERTIES OF HADRONS

B. Krusche

*Department of Physics and Astronomy, University of Basel, Klingelbergstr. 82
CH-4056 Basel, Switzerland
Bernd.Krusche@unibas.ch*

Received Day Month Year

Revised Day Month Year

A diverse experimental program for the study of the photoproduction of mesons off nuclei has been carried out - and is still running - at the Mainz MAMI and Bonn ELSA electron accelerators with the TAPS, Crystal Barrel, and Crystal Ball calorimeters. It is motivated as a detailed study of the in-medium properties of hadrons and the meson - nucleus interactions. Typical examples for the in-medium behavior of vector mesons (ω), scalar mesons (σ), and nucleon resonances ($P_{33}(1232)$, $S_{11}(1535)$, $D_{15}(1520)$) are discussed. Special attention is paid to meson - nucleus final state interactions.

Keywords: Hadron in-medium properties; Photoproduction of mesons from nuclei

PACS numbers: 13.60.Le, 25.20.Lj, 21.65+f

1. Introduction

In-medium properties of hadrons are a hotly debated topic since they are closely related to the properties of low-energy, non-perturbative QCD. Unlike any other composite systems, hadrons are objects, which are build out of constituents with masses (5 - 15 MeV for u,d quarks) that are negligible compared to the total mass. Most of the mass is generated by dynamical effects from the interaction of the quarks and an important role is played by the spontaneous breaking of chiral symmetry, the fundamental symmetry of QCD. The symmetry breaking, which is connected to a non-zero expectation value of scalar $q\bar{q}$ pairs in the vacuum, the chiral condensate, is reflected in the hadron spectrum. Without it, hadrons would appear as mass degenerate parity doublets, which is neither true for baryons nor for mesons. However, model calculations (see e.g. Ref 1) indicate a temperature and density dependence of the condensate, which is connected with a partial restoration of chiral symmetry. Although there is no direct relation between the quark condensate and the in-medium properties of hadrons (masses, widths etc.), there is an indirect one via QCD sum rules, which connect the QCD picture with the hadron picture. In the latter, the in-medium modifications arise from the coupling of mesons to resonance - hole states and the coupling of the modified mesons to resonances. The best known example is the treatment of the Δ in the framework of the Δ -hole model

2 *B. Krusche*

(see e.g. Ref. 2, 3). Recently, Post, Leupold, and Mosel⁴ have calculated the hadron in-medium spectral functions for π^- , η^- , and ρ -mesons and baryon resonances in a self-consistent coupled channel approach. The relevant diagrams for the vacuum

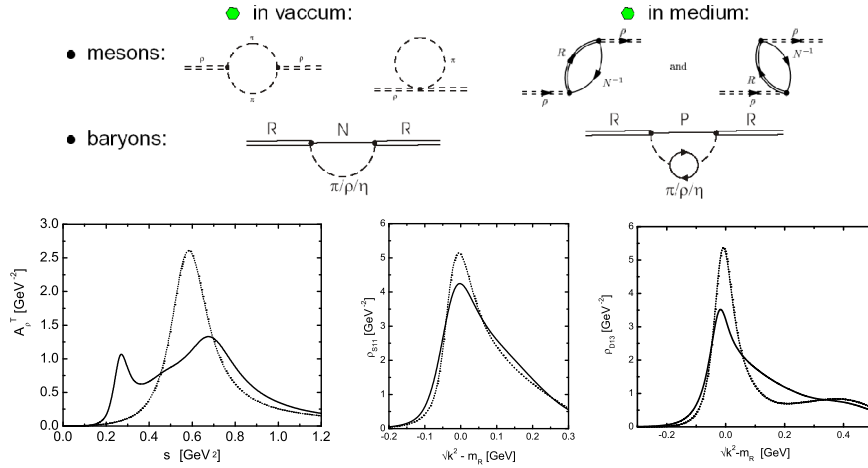


Fig. 1. Upper part: diagrams for the vacuum and in-medium self-energies of mesons and baryons.⁴ Lower part: predicted vacuum (dashed curves) and in-medium (solid curves) spectral functions for the ρ -meson (left), the $S_{11}(1535)$ (center), and the $D_{13}(1520)$ (right) resonances at $q=0$.⁴

and in-medium self-energies and typical results for the spectral functions are shown in Fig. 1. In case of the resonances, the largest effects are predicted for the D_{13} , due to the strong coupling of this resonance to the $N\rho$ channel.

The experimental investigation of hadron in-medium properties is complicated by initial (ISI) and/or final (FSI) state interactions. Since the experiments discussed here use photoproduction of mesons, no ISI but significant FSI effects must be considered. However, the investigation of this reactions allows also a detailed study of the meson - nucleus interactions, which are responsible for the FSI.⁶⁻⁸ The simplest information comes from the mass number scaling of the meson production cross sections, which can be parameterized by $\sigma(A) \propto A^\alpha$. Qualitatively, $\alpha \approx 2/3$ corresponds to strong absorption (cross section proportional to nuclear surface) and $\alpha \approx 1$ to negligible absorption (cross section proportional to nuclear volume). The scaling for different meson production channels has been discussed in detail in Refs. 7, 8. Fig. 2 shows the coefficient α for π^- - and η mesons as function of their momentum. The absorption of pions is strong in the range where the Δ resonance can be excited (around 200 MeV), but nuclear matter becomes almost transparent for pions below momenta of 100 MeV. The absorption of η mesons is already large for very low momenta, since the S_{11} resonance is located at the η production threshold. Quantitatively, one can convert the coefficients into absorption cross sections and mean free paths e.g. via Glauber theory (see e.g. Ref. 6).

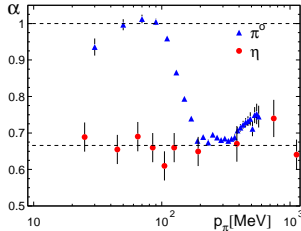


Fig. 2. Scaling coefficient α derived from a fit of $\sigma(A) \propto A^\alpha$ to data from carbon, calcium, niobium and lead nuclei, as function of meson momentum for π^0 - and η -mesons.⁵⁻⁷

An extensive program for the investigation of meson photoproduction reactions off nuclei has been carried out at the Mainz MAMI and Bonn ELSA accelerators with the TAPS^{9,10} and Crystal Barrel detectors¹¹. It included the following topics:

- The search for in-medium modifications of vector mesons via the investigation of the resonance shape of the ω meson from its $\pi^0\gamma$ decay.¹²
- The study of the pion-pion invariant mass distributions for $2\pi^0$ and $\pi^0\pi^\pm$ photoproduction as a tool for the in-medium behavior of the σ meson.^{13,14}
- Resonance contributions to η , π , 2π meson production reactions from nuclei, aiming at the in-medium properties of nucleon resonances.^{5-8,15,18}
- The search for η -nucleus bound states (η mesic nuclei).^{16,17}
- The investigation of η , $2\pi^0$, and η' photoproduction off light nuclei for the study of the excitation of resonances of the neutron.¹⁹⁻²⁴

2. In-Medium Modifications of Mesons

2.1. Vector mesons: the ω -meson

In-medium modifications of vector mesons have been searched for via the spectroscopy of di-lepton pairs in heavy ion reactions by the CERES experiment^{25,26} and more recently the NA60 collaboration²⁷, which reported an in-medium broadening of the ρ . In-medium modifications of ρ and ω mesons were reported from 12 GeV p+A reactions at KEK²⁸. Recently, a modification of the Φ meson has been suggested on the basis of the A -dependence of the photoproduction yields.²⁹

The CBELSA/TAPS¹² experiment measured the line shape of the $\omega \rightarrow \pi^0\gamma$ invariant mass peak off the free proton and off nuclei. The measured invariant mass peaks of the $\pi^0 \rightarrow \gamma\gamma$, $\eta \rightarrow 3\pi^0 \rightarrow 6\gamma$, and $\eta' \rightarrow \pi^0\pi^0\eta \rightarrow 6\gamma$ decays were identical for hydrogen and the nuclear targets. Only in case of the ω a low energy shoulder of the peak was found for nuclei (see Fig. 3). Due to its life time, only a small fraction of the ω 's decay in the medium, so that also the nuclear invariant mass peaks include a dominant contribution of unmodified in-vacuum decays. This is reflected in the data since the low-energy tail of the invariant mass stems almost exclusively from ω 's with small momenta, which have the largest change for in-medium decays. The peak centroids as function of the momentum are shown in Fig. 3, right hand side. Similar results were found for carbon, an analysis of the A scaling of the production cross sections is under way, and a second generation experiment is approved.

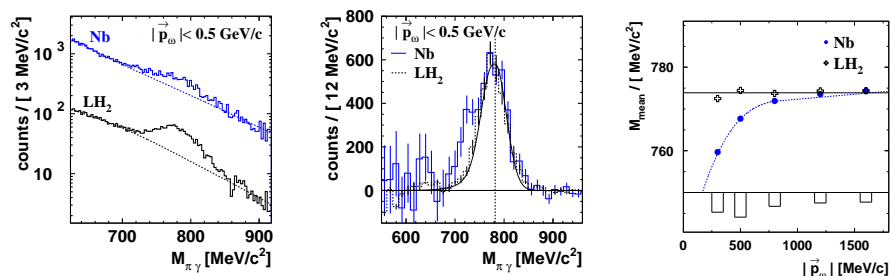
4 *B. Krusche*


Fig. 3. ω invariant mass peak. Left: comparison invariant mass spectra niobium - proton, center: after subtraction of (combinatorial) background, right: momentum dependence of peak centroid.¹²

2.2. Scalar mesons: the σ -meson

A very interesting case is the mass-split between the $J^\pi=0^-$ pion and the $J^\pi=0^+$ σ -meson. The naive assumption, that the two masses should become degenerate in the chiral limit is supported by model calculations. A typical result is the density dependence of the mass calculated in the Nambu-Jona-Lasino model³⁰ (see Fig. 4). The nature of the σ meson itself has been much discussed in the literature. The review of particle properties³¹ lists as σ the $f_0(600)$ with a mass of 400 - 1200 MeV and a full width between 600 MeV - 1000 MeV. Precise predictions for mass and width from dispersion relations were derived in Ref. 32. In some approaches the σ is treated as a pure $q\bar{q}$ (quasi)bound state^{30,33,34}, in others as a correlated $\pi\pi$ pair in a $I = 0$, $J^\pi = 0^+$ state³⁵⁻³⁷. But in any case a strong coupling to scalar, iso-scalar pion pairs is predicted. As a consequence, all models predict a downward shift of the strength in the invariant mass distributions of such pion pairs in the medium. This is either due to the in-medium spectral function of the σ meson³³ or the modification of the pion-pion interaction³⁶ due to the coupling to nucleon - hole, Δ - hole and N^* - hole states.

First experimental evidence has been reported by the CHAOS collaboration from pion induced double pion production.³⁸⁻⁴² They found a build-up of strength with rising mass number at low invariant masses for the $\pi^+\pi^-$ final state, but not for the $\pi^+\pi^+$ channel where the neutral σ meson cannot contribute. A similar effect was found in the $\pi^- A \rightarrow A\pi^0\pi^0$ reaction with Crystal Ball at BNL.⁴³

In contrast to pion induced reactions, photoproduction reactions avoid initial state interactions, although also in this case FSI complicates the picture. FSI can be minimized by the use of low incident photon energies, giving rise to low-energy pions which have large mean free paths⁷ (see Fig. 2). Photoproduction of pion pairs at low incident photon energies off the free proton and the quasifree neutron has been previously studied with the DAPHNE⁴⁴⁻⁴⁸ and TAPS^{20,22,49-52} detectors at MAMI in Mainz (see Ref. 53 for an overview). First results from a measurement of double π^0 and $\pi^0\pi^\pm$ photoproduction off carbon and lead have been reported in

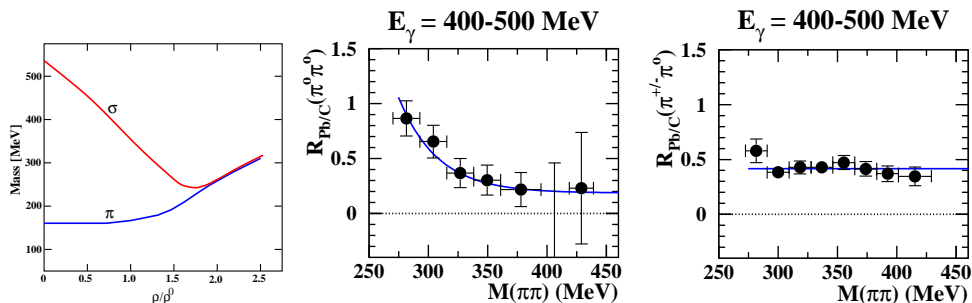


Fig. 4. Left hand side: predicted density dependence of π and σ mass³⁰, center (right hand side): measured $R_{Pb/C}$ ratio for $\pi^0\pi^0$ ($\pi^\pm\pi^0$).¹³

Ref. 13. For the heavier nucleus a shift of the strength to lower invariant masses was found for the $\pi^0\pi^0$ channel but not for the mixed charge channel. This is particularly clearly seen in the normalized ratios of the invariant mass distributions defined by

$$R_{(Pb/C)}(\pi^0\pi^0) = \frac{d\sigma_{Pb}(\pi^0\pi^0)}{\sigma_{Pb}(\pi^0\pi^0)dM} \bigg/ \frac{d\sigma_C(\pi^0\pi^0)}{\sigma_C(\pi^0\pi^0)dM} \quad (1)$$

and analogously for $R_{(Pb/C)}(\pi^0\pi^\pm)$. The results are shown in Fig. 4, center and right hand side. The ratio rises for the double π^0 production, but is almost constant for the mixed charge channel. This behavior was used as an argument, that the effect does not arise from FSI, which was assumed to be similar for neutral and charged pions. In the meantime, also data for the medium-weight nucleus ^{40}Ca became available¹⁴ (see Fig. 5), which is discussed below.

A quantitative interpretation of the distributions requires models which account for the ‘trivial’ in-medium effects, like the momentum distributions of the bound nucleons and FSI of the pions. Recently Mühlich et al.^{54,55} and Buss et al.⁵⁶ have performed detailed calculations of the nuclear double pion photoproduction reactions in the framework of coupled channel transport models based on the semi-classical Boltzmann-Uehling-Uhlenbeck (BUU) equation. Special emphasis was laid on the description of the scattering and absorption properties of low energy pions. An important result of this model is, that even without explicit in-medium modification of the $\pi^0\pi^0$ channel, the respective invariant mass distributions show a softening for heavy nuclei. This effect arises solely from FSI of the pions. The πN absorption cross section increases with pion kinetic energy, so that pions with large momenta are more strongly depleted via the $\pi N \rightarrow \Delta$, $\Delta N \rightarrow NN$ reaction path. But this causes only part of the effect. Important are also re-scattering processes, which tend to decrease the pion kinetic energy and thus the average pion - pion invariant mass. This effect is enhanced due to charge exchange scattering. Since the total cross section for $\pi^0\pi^\pm$ production is much larger than the $\pi^0\pi^0$ cross section, the latter receives significant side feeding from the mixed charge channel via $\pi^\pm N \rightarrow N\pi^0$ scattering. Consequently, the relative softening of the $\pi^0\pi^0$ invariant

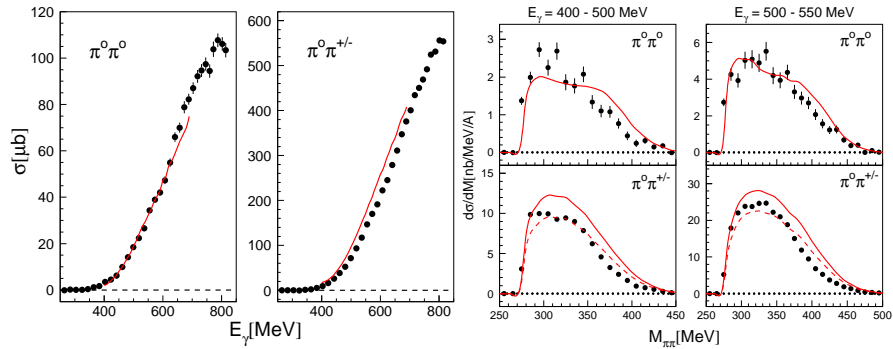
6 *B. Krusche*


Fig. 5. Double pion production off ^{40}Ca . Left hand side: total cross sections, right hand side: invariant mass distributions. Data from Ref. 14, curves: BUU results⁵⁶ (dashed: re-scaled to data).

mass by itself is no safe evidence for an in-medium modification of the pion - pion interaction.

The overall agreement between the model results and the measured total cross sections (see fig. 5) is excellent for the $\pi^0\pi^0$ channel. The data for the mixed charge channel are a slightly overestimated by the model, however, this is within the systematic uncertainty. The general tendency of a softening of the invariant mass distributions is reproduced by the calculations as a consequence of FSI effects. On a quantitative level, the data for the $\pi^0\pi^0$ invariant masses for the lowest incident photon energies seem to be somewhat stronger downward shifted than predicted. This is the energy range where the smallest FSI effects are expected.

The search for the possible in-medium modification of the pion - pion interaction, respectively the σ in-medium modification, thus becomes a quantitative question. At least part of the observed effect is due to pion final state interaction. Further efforts are needed to clarify, if there are effects beyond what can be explained by BUU. To this end, data with much higher statistical quality, in particular for lead, have been recently measured with the Crystal Ball/TAPS detector at MAMI.

3. In-Medium Modifications of Nucleon Resonances

Nucleon resonances in the medium are effected by the Pauli-blocking of final states, which decreases their width, additional decay channels like $RN \rightarrow NN$ (R = resonance, N = nucleon), which cause collisional broadening, and as already discussed in the introduction, by the coupling to mesons with medium-modified properties.

3.1. The Δ resonance

The excitation of the Δ and its propagation through the nuclear medium have been studied in different reactions, an in-medium broadening at normal nuclear matter density of ≈ 100 MeV has been extracted. In this sense the Δ is a well understood

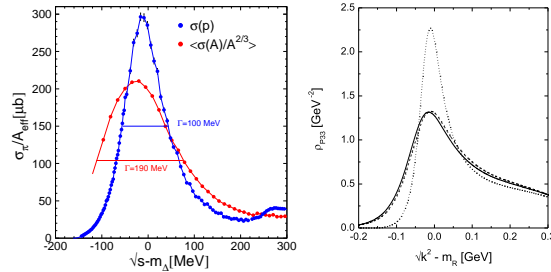


Fig. 6. Left hand side: total π^0 photoproduction of the proton and the average for heavy nuclei¹⁵. Right hand side: self-consistent spectral functions in-vacuum and in-medium for the $\Delta(1232)$ ⁴.

test case. However, a detailed understanding of the Δ case is also important for the interpretation of meson production reactions in the higher nucleon resonance regions, where the Δ contributes indirectly e.g. via multiple pion production processes and through re-absorption of pions. The line shape of the Δ measured with photoproduction of π^0 mesons off the free proton and off nuclei^{7,15} is compared in Fig. 6 to the spectral functions calculated in Ref. 4. Both, data and model show an in-medium broadening of the Δ close to 100 MeV. This is also in agreement with a study of coherent π^0 photoproduction of heavy nuclei, which allowed a more detailed investigation of the Δ in-medium properties⁵⁸.

3.2. The second resonance region

The second resonance region is composed of the $P_{11}(1440)$, $D_{13}(1520)$, and $S_{11}(1535)$ states. A significant in-medium modification of the D_{13} is predicted due to the strong coupling to $N\rho$, while only small effects are expected for the S_{11} (see Fig. 1)⁴. The experimental finding from total photoabsorption is, that the second resonance bump is completely suppressed for all nuclei from beryllium onwards.⁵⁹ However, total photoabsorption does not give any information about the behavior of individual resonances. Photoproduction of η mesons in this energy range is completely dominated by the S_{11} resonance^{60–64}, while single π^0 , double π^0 and $\pi^0\pi^\pm$ photoproduction^{49–51,65} show a clear signal for the D_{13} resonance. These reactions are therefore well suited for the study of the in-medium properties of this resonances.

Photoproduction of η mesons off nuclei had been previously studied up to 800 MeV incident photon energy with TAPS at MAMI⁶ and for energies up to 1.1 GeV at KEK⁶⁶ and Tohoku⁶⁷. The first experiment found no in-medium broadening of the resonance (beyond effects from Fermi smearing and η FSI), the KEK experiment reported some collisional broadening of the resonance and the Tohoku experiment pointed to a significant contribution of a higher lying resonance to the $\gamma n \rightarrow n\eta$ reaction. However, none of these experiments covered the full line shape of the S_{11} .

Preliminary results for η photoproduction off the deuteron and off nuclei from the

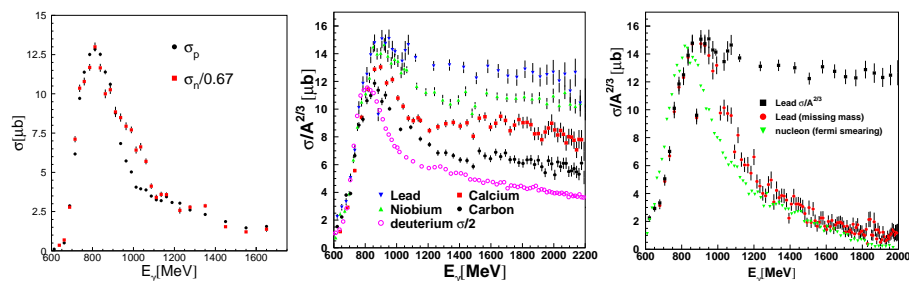
8 *B. Krusche*


Fig. 7. Left: preliminary result for the total $\gamma p \rightarrow p\eta$ and $\gamma n \rightarrow n\eta$ cross sections measured off quasifree nucleons from the deuteron. Center: inclusive $\gamma A \rightarrow \eta X$ cross sections for the deuteron, carbon, calcium, niobium and lead. Right: Inclusive cross section and single η production cross sections for lead compared to the Fermi smeared average nucleon cross section.

Crystal Barrel/TAPS experiment at the Bonn ELSA accelerator are summarized in Fig. 7. The measurement off quasifree nucleons from the deuteron (coincident detection of recoil nucleons) shows that indeed the elementary neutron cross section has a bump-like structure (see Fig. 7, left hand side) corresponding to a higher lying nucleon resonance. As already reported in Ref. 6, the inclusive nuclear cross sections scale like $A^{2/3}$ for incident photon energies below 800 MeV. They behave differently at higher incident photon energies (see Fig. 7, center) where $\eta\pi$ final states and secondary production mechanisms (e.g. $\gamma N \rightarrow N\pi$, $\pi N \rightarrow \eta N$) contribute and obscure the S_{11} line shape. This contributions can be almost completely suppressed by cuts on the reaction kinematics. After these cuts, single η photoproduction off heavy nuclei like lead (see Fig. 7, right hand side) becomes very similar to the Fermi smeared average nucleon cross section. The small discrepancy is at least partly due to inefficiencies of the kinematical cuts.

Preliminary results for double pion photoproduction are summarized in Fig. 8. Results for double π^0 and $\pi^0\pi^\pm$ have been obtained¹⁴ for incident photon energies up to 800 MeV (see Fig. 8, left hand side). In case of double π^0 , the excitation functions off the deuteron and off ^{40}Ca have exactly the same shape so that there is no indication for an in-medium modification of the D_{13} at energies below its peak position. However, the model⁴ (see Fig. 1) predicts the main effect for the high energy tail of the resonance. This part is covered by the preliminary data from the Crystal Barrel/TAPS experiment (see Fig. 8, right hand side), which indeed shows a difference between deuteron and nuclear data, in particular in the 'dip'-region between the second and third resonance bump.

Even more interesting than the double π^0 channel would be the $\pi^0\pi^\pm$ final state. This is so, because as shown in Ref. 68 the signal for in-medium modifications of resonances is strongly diluted by the averaging over the nuclear volume for decay channels that are not directly responsible for the modification. The main effect for the D_{13} is connected with the coupling to the $N\rho$ channel, and only the mixed charge double pion decay can proceed via an intermediate ρ (the $\rho^0 \rightarrow \pi^0\pi^0$ decay

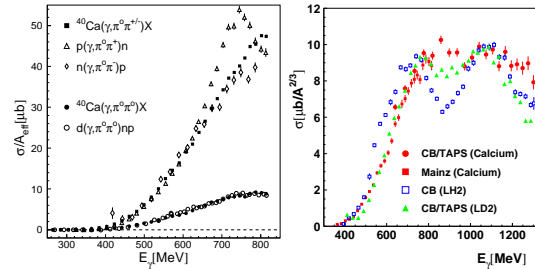


Fig. 8. Left hand side: Total cross sections for $\pi^0\pi^0$ and $\pi^0\pi^\pm$ photoproduction off ^{40}Ca compared to $d(\gamma, \pi^0\pi^0)np$ ²² respectively to $p(\gamma, \pi^0\pi^+)n$ ⁵¹ and $n(\gamma, \pi^0\pi^-)p$ ⁴⁵. Cross sections normalized to $A_{eff} = A^{2/3}$ for calcium and $A_{eff} = A$ for $A = 1, 2$. Right hand side: total cross sections for double π^0 off proton, deuteron and ^{40}Ca (preliminary).

is forbidden). Unfortunately, so far only data up to 800 MeV are available (see Fig. 8, left hand side). However, even in this region there is already a significant difference in the excitation functions off the free proton and off ^{40}Ca . The peak-like structure for the proton is suppressed in the nuclear data, but the same is true for the quasifree neutron cross section extracted from deuteron data⁴⁵. Data over a wider energy range and a comparison of quasifree data off the bound proton to the bound neutron will be necessary to clarify this issue.

Acknowledgments

The discussed results have been obtained by the TAPS-collaboration at MAMI and the Crystal Barrel/TAPS collaboration at ELSA. They are part of the theses works of D. Trnka (U. Giessen) and F. Bloch, I. Jaegle, and Th. Mertens (U. Basel). This work was supported by Schweizerischer Nationalfonds.

References

1. M. Lutz, S. Klimt, and W. Weise, *Nucl. Phys.* **A542**, 521 (1992).
2. E. Oset and W. Weise, *Nucl. Phys.* **A402**, 612.
3. J.H. Koch and E.J. Moniz, *Phys. Rev.* **C27** 751.
4. M. Post, S. Leupold, and U. Mosel, *Nucl. Phys.* **A741**, 81 (2004).
5. Th. Mertens, *PhD thesis, University of Basel 2006, to be published*.
6. M. Rößig-Landau et al., *Phys. Lett.* **B373** (1996) 45.
7. B. Krusche et al., *Eur. Phys. J.* **A22**, 277 (2004).
8. B. Krusche et al., *Eur. Phys. J.* **A22**, 347 (2004).
9. R. Novotny, *IEEE Trans. on Nucl. Science* **38**, 379 (1991).
10. A.R. Gabler et al., *Nucl. Instr. and Meth.* **A346**, 168 (1994).
11. E. Aker et al., *Nucl. Instr. and Meth.* **A321**, 69 (1992).
12. D. Trnka et al., *Phys. Rev. Lett.* **94**, 192303 (2005).
13. J.G. Messchendorp et al., *Phys. Rev. Lett.* **89**, 222302 (2002).
14. F. Bloch et al., *submitted to Eur. Phys. J. A* (2006).
15. B. Krusche, *Prog. Part. Nucl. Phys.* **55**, 46 (2005).
16. V. Hejny et al., *Eur. Phys. J.* **A13**, 493 (2004).

10 *B. Krusche*

17. M. Pfeiffer et al., *Phys. Rev. Lett.* **92**, 252001 (2004).
18. B. Krusche et al., *Phys. Rev. Lett.* **86**, 4764 (2001).
19. B. Krusche et al., *Phys. Lett.* **B358**, 40 (1995).
20. B. Krusche et al., *Eur. Phys. J.* **A6**, 309 (1999).
21. V. Hejny et al., *Eur. Phys. J.* **A6** 83 (1999).
22. V. Kleber et al., *Eur. Phys. J.* **A9**, 1 (2000).
23. J. Weiss et al., *Eur. Phys. J.* **11** 371 (2001).
24. J. Weiss et al., *Eur. Phys. J.* **16** 275 (2003).
25. G. Agakichiev et al., *Phys. Rev. Lett.* **75**, 1272 (1995).
26. D. Adamova et al., *Phys. Rev. Lett.* **91**, 042301 (2003).
27. S. Damjanovic et al., *nucl-ex/0510044*.
28. M. Naruki et al., *Phys. Rev. Lett.* **96**, 092301 (2006).
29. T. Ishikawa et al., *Phys. Lett.* **B608**, 215 (2005).
30. V. Bernard, U.-G. Meiner, and I. Zahed, *Phys. Rev. Lett.* **59**,) 966 (1987).
31. S. Eidelmann et al., *Phys. Lett.* **B592**, 1 (2004).
32. I. Caprini, G. Colangelo, and H. Leutwyler, *Phys. Rev. Lett.* **96**, 132001 (2006).
33. T. Hatsuda, T. Kunihiro, and H. Shimizu, *Phys. Rev. Lett.* **82**, 2840 (1999).
34. Z. Aouissat, G. Chanfray, P. Schuck, and J. Wambach, *Phys. Rev.* **C61**, 012201 (2000).
35. H.C. Chiang et al., *Nucl. Phys.* **A644**, 77 (1998).
36. L. Roca, E. Oset, and M.J. Vicente Vacas, *Phys. Lett.* **B541**, 77 (2002).
37. G. Chanfray et al., *Eur. Phys. J.* **A27**, 191 (2006).
38. F. Bonutti et al., *Phys. Rev. Lett.* **77**, 603 (1996).
39. F. Bonutti et al., *Phys. Rev.* **C 60**, 018201 (1999).
40. F. Bonutti et al., *Nucl. Phys.* **A 677**, 213 (2000).
41. P. Camerini et al., *Nucl Phys.* **A735**, 89 (2004).
42. N. Grión et al., *Nucl. Phys.* **A763**, 80 (2005).
43. A. Starostin et al., *Phys. Rev. Lett.* **85**, 5539 (2000).
44. A. Braghieri et al., *Phys. Lett.* **B363**, 46 1995.
45. A. Zabrodin et al., *Phys. Rev.* **C55**, R1617 (1997), and P. Pedroni *priv. com.*
46. A. Zabrodin et al., *Phys. Rev.* **C60**, 055201 (1999).
47. J. Ahrens et al., *Phys. Lett.* **B551**, 49 (2003).
48. J. Ahrens et al., *Phys. Lett.* **624**, 173 (2005).
49. F. Härter et al., *Phys. Lett.* **B401**, 229 (1997).
50. M. Wolf et al., *Eur. Phys. J.* **A9**, 5 (2000).
51. W. Langgärtner et al., *Phys. Rev. Lett.*, **87** 052001 (2001).
52. M. Kotulla et al., *Phys. Lett.* **B578**, 63 (2004).
53. B. Krusche and S. Schadmand, *Prog. Part. Nucl. Phys.* **51**, 399 (2003).
54. P. Muehlich et al., *Phys. Rev.* **C67**, 024605 (2003).
55. P. Muehlich et al., *Phys. Lett.* **B595**, 216 (2004).
56. O. Buss et al., *nucl-th/0603003*, and *private communication* (2006).
57. M. Hirata et al., *Ann. Phys.* **120** 205 (1979).
58. B. Krusche et al. *Phys. Lett.* **B526**, 287 (2002).
59. N. Bianchi et al., *Phys. Lett.* **B325**, 249 (1994).
60. B. Krusche et al., *Phys. Rev. Lett.* **74**, 3736 (1995).
61. B. Krusche et al., *Phys. Lett.* **B397**, 171 (1997).
62. F. Renard et al., *Phys. Lett.* **B528**, 215 (2002).
63. M. Dugger et al., *Phys. Rev. Lett.* **89**, 222002 (2002).
64. V. Crede et al., *Phys. Rev. Lett.* **94**, 012004 (2005).
65. O. Bartholomy et al., *Phys. Rev. Lett.* **94**, 012003 (2005).
66. T. Yorita et al., *Phys. Lett.* **B476**, 226 (2000).

67. T. Kinoshita et al., *Phys. Lett.* **B639**, 429 (2006).
68. J. Lehr and U. Mosel, *Phys. Rev.* **C64**, 042202. (2001).